Tribol Lett (2014) 55:15–21
DOI 10.1007/s11249-014-0327-y

ORIGINAL PAPER

Rolling Friction: Comparison of Analytical Theory with Exact Numerical Results

Michele Scaraggi · Bo N. J. Persson

Received: 21 November 2013 / Accepted: 26 March 2014 / Published online: 18 April 2014

Abstract We study the contact mechanics of a smooth hard cylinder rolling on a flat surface of a linear viscoelastic solid. Using the measured viscoelastic modulus of unfilled and filled (with carbon black) nitrile rubber, we compare numerically exact results for the rolling friction with the prediction of a simple analytical theory. For the unfilled rubber, the two theories agree perfectly while some small difference exists for the filled rubber. The rolling friction coefficient depends nonlinearly on the normal load and the rolling velocity.

Keywords Rubber friction · Rolling friction · Polymer · Viscoelasticity

1 Introduction

Rubber friction is a topic of huge practical importance, e.g., for tires, rubber seals, wiper blades, conveyor belts, and syringes [1–16]. Many experiments have been performed with a hard sphere or cylinder rolling on a flat rubber substrate [17–20]. Nearly the same friction force may be observed during sliding as during rolling, assuming that the interface is lubricated and that the sliding velocity and fluid viscosity are such that a thin lubrication film is formed with a thickness much smaller than the indentation depth of the ball, but larger than the amplitude of the roughness on the surfaces [17]. The results of rolling friction experiments have often been analyzed using a very simple model of Greenwood and Tabor [17], which, however, contains a (unknown) factor α, representing the fraction of the input elastic energy lost as a result of the internal friction of the rubber.

Several (analytical) theoretical studies have been presented for the rolling and sliding friction involving viscoelastic solids, which, however, are based on a simplified description of the rubber rheology, i.e., on a single term Prony series. The case of cylinder contact has been analytically treated by Hunter [21] and Goriacheva [22], and the approach lately approximately extended to the case of three-dimensional contact by enforcing a two-dimensional reduction in the problem [23]. However, the relaxation spectrum of real polymers is usually very wide and the rolling friction of real rubber compounds cannot be predicted using those existing exact theories. This limitation also applies to recent numerical models based on the efficient boundary element formulation of the contact problem [24], where the single relaxation time rheology is adopted.

Recently, one of us (BNJP) has developed a Fourier series-based approach for the prediction of rolling friction for real rubber materials [25]. This approach, accurate to linear order in the loss tangent, is able to predict quantitatively reliable results, as shown for both line [25] (see also in the following) and point contacts [26], with negligible computational effort. The theory can be applied to solids with arbitrary viscoelastic modulus. For a cylinder rolling on a viscoelastic solid characterized by a single relaxation time, Hunter [21] has obtained an exact result for the rolling friction, and the analytical theory [25] agrees very well with the result of Hunter. Unfortunately, the approach in Ref. [25] does not allow us to determine the traction and the displacement fields occurring at the contact.

M. Scaraggi (✉) · B. N. J. Persson
Peter Grünberg Institut-1,FZ-Jülich, 52425 Jülich, Germany
e-mail: michele.scaraggi@unisalento.it

B. N. J. Persson
e-mail: b.persson@fz-juelich.de

M. Scaraggi
DII, Universitá del Salento, 73100 Monteroni-Lecce, Italy

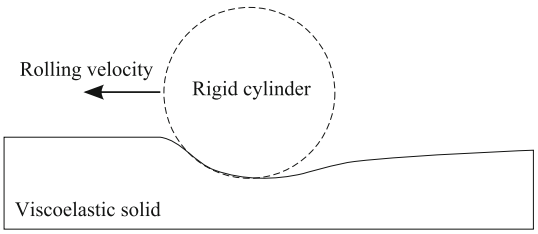

Fig. 1 Smooth rigid cylinder in steady rolling contact with a viscoelastic solid with nominally flat surface. Schematic

Full numerical solutions of the viscoelastic contact problem, of interest for many tribological applications, have only very recently been presented for smooth and rough contacts, see e.g., Ref. [26]. This should not surprise at all, due to the numerical complexity of the underlying problem, which is even more pronounced in case of real (multiscale) rough contacting surfaces. As a result, the hysteretic rubber friction coming from local sliding contacts can be, nowadays, only effectively calculated based on homogenized contact mechanics theories [3].

In this study, we compare the analytical theory of Ref. [25] with exact numerical results. In particular, in Sect. 2, we describe our numerical approach; in Sect. 3, we briefly describe the analytical approach of Ref. [25] as applied to cylinder on flat. Section 4 presents the numerical comparison of the two models. Section 5 contains the summary and conclusion.

2 Rolling Friction: Numerical Theory

We consider the line contact case with a rigid cylinder, with perfectly smooth surface, rolling on an isotropic viscoelastic half-space, see Fig. 1. In order to determine the surface deformation of the viscoelastic half-space, we assume that quasi-static bulk dynamics holds, i.e., inertia effects are neglected. If a stress $\sigma_z(\mathbf{x},t)$ acts on the surface of a semi-infinite viscoelastic solid, it will result in a normal surface displacement $u_z(\mathbf{x},t)$. The latter is linearly related to $\sigma_z(\mathbf{x},t)$ via an equation which is particular simple when the spatial and time coordinates are Fourier transformed [3]:

$$u_z(\mathbf{q},\omega) = M_{zz}(\mathbf{q},\omega)\sigma_z(\mathbf{q},\omega), \tag{1}$$

where

$$M_{zz}(\mathbf{q},\omega) = -\frac{2(1-\nu^2)}{qE(\omega)}, \tag{2}$$

and where $E(\omega)$ is the frequency-dependent (complex) Young's modulus. In what follows, we will assume that the Poisson's ratio $\nu(\omega)$ is independent of frequency. This assumption is a good approximation in most cases (see e.g., Ref. [25]), and it means that the dynamics of relaxation in orthogonal directions proceeds equally in time. If a rigid cylinder is sliding in steady state on a semi-infinite rubber solid, we have

$$\sigma_z(\mathbf{x},t) = \sigma_z(\mathbf{x}-\mathbf{v}t)$$

which gives

$$\sigma_z(\mathbf{q},\omega) = \delta(\mathbf{q}\cdot\mathbf{v}-\omega)\sigma_z(\mathbf{q}). \tag{3}$$

For the cylinder geometry with the cylinder axis along the y-direction, $\sigma_z(\mathbf{x})$ is independent of y, and we write $\sigma_z(\mathbf{x}) = -p(x)$ so that

$$\sigma_z(\mathbf{q}) = -p(q_x)\delta(q_y). \tag{4}$$

Using (1)–(4) gives

$$u_z(\mathbf{q},\omega) = \frac{2(1-\nu^2)}{|q_x|E(\omega)}p(q_x)\delta(q_y)\delta(q_x v_x-\omega).$$

Thus, we get:

$$\begin{aligned} u_z(x,t) &= \int \mathrm{d}^2q\mathrm{d}\omega\; u_z(\mathbf{q},\omega)e^{i(\mathbf{q}\cdot\mathbf{x}-\omega t)} \\ &= \int \mathrm{d}\omega\frac{2(1-\nu^2)}{|\omega|E(\omega)}p(\omega/v_x)e^{i\omega(x/v_x-t)}. \end{aligned} \tag{5}$$

Now because of causality, one can write

$$\frac{1}{E(\omega)} = \frac{1}{E(\infty)} + \int_0^\infty \mathrm{d}\tau\frac{H(\tau)}{1-i\omega\tau}, \tag{6}$$

where the spectral density $H(\tau)$ is a positive real function of the rubber relaxation time τ. Note that we can also write

$$\frac{1}{E(\omega)} = \frac{1}{E(\infty)}\left[1 + \int_0^\infty \mathrm{d}t\;\Gamma(t)e^{i\omega t}\right], \tag{7}$$

where

$$\Gamma(t) = E(\infty)\int_0^\infty d\tau\,\frac{H(\tau)}{\tau}e^{-t/\tau}.$$

We write

$$p(q_x) = \frac{1}{2\pi}\int dx'\;p(x')e^{-iq_x x'}. \tag{8}$$

Substituting (7) and (8) in (5) gives

$$\begin{aligned} u_z(x,t) = \frac{(1-\nu^2)}{\pi E(\infty)}\int \mathrm{d}x'\int \mathrm{d}\omega\,\frac{1}{|\omega|}p(x') \\ \times\left[e^{i\alpha\omega/v_x} + \int_0^t \mathrm{d}t'\;\Gamma(t')e^{i\beta(t')\omega/v_x}\right], \end{aligned} \tag{9}$$

where $\alpha = x - x' - v_x t$ and $\beta(t') = x - x' - v_x(t - t')$. Now consider the integral

$$J = \int_{-\infty}^{\infty} \mathrm{d}\omega \, \frac{1}{|\omega|} e^{i\alpha\omega/v_x}.$$

We write $\omega/v_x = q_\mathrm{x}$ and get

$$J = 2\int_0^{\infty} \mathrm{d}q_\mathrm{x} \, \frac{\cos(\alpha q_\mathrm{x})}{q_\mathrm{x}}.$$

This integral diverges. The problem arises from the small wavevector region $q_\mathrm{x} \to 0$ and reflects the infinite size of the system. For a finite (but very large) solid with linear dimension L, we must replace the lower integration limit with π/L, so that

$$J = 2\int_{\pi/L}^{\infty} \mathrm{d}q_\mathrm{x} \frac{\cos(\alpha q_\mathrm{x})}{q_\mathrm{x}}.$$

Let us denote $|\alpha| q_\mathrm{x} = \xi$ so that

$$J = 2\int_{|\alpha|\pi/L}^{\infty} \mathrm{d}\xi \, \frac{\cos\xi}{\xi}.$$

For large (but fixed) L, this will give

$$J \approx \text{const.} - 2\log|\alpha|.$$

Using this result in (9) gives

$$u_\mathrm{z}(x,t) = u_0 - \frac{2(1-\nu^2)}{\pi E(\infty)} \int \mathrm{d}x' \, p(x') \times \Big[\log|x - x' - v_\mathrm{x} t| + \int_0^t \mathrm{d}t' \, \Gamma(t') \log|x - x' - v_\mathrm{x}(t - t')|, \Big]$$

where u_0 is a constant. In what follows, we study the system in a coordinate system fixed to the cylinder which correspond to replacing $x \to x + v_x t$. We also denote the velocity of the cylinder with $v_x = v_0$ and the high-frequency modulus $E(\infty)$ with E_∞. We consider long times $t \to \infty$ where the sliding is steady state, where $u(x,t) = u(x)$ (in the moving reference frame) is time independent. With these assumptions, we get

$$u_z(x) = u_0 - \frac{2(1-\nu^2)}{\pi E_\infty} \int dx' \, p(x') \times \left[\log|x - x'| + \int_0^{\infty} dt' \, \Gamma(t') \log|(x - x' - v_0 t')|\right]. \tag{10}$$

Eq. (10) is based on a Green's function formulation of the bulk viscoelastic deformation problem, similarly to Ref. [26]. The derivation above is for a homogeneous viscoelastic half-space, but can be easily generalized to a layered material, which introduce in (2) an additional factor $S(q,\omega)$ which is known analytically (see e.g., Ref. [27]). In this work, differently from what reported in Ref. [26], the line contact condition allows us to derive an exact discrete formulation of Eq. (10) [28], hence avoiding numerical issues coming from its integration over a wide range of relaxation times describing real rubbers.

The rolling friction coefficient:

$$\mu_\mathrm{R} = -\frac{1}{f_\mathrm{N}} \int dx \, p(x) h'(x),$$

where $h(x) = \text{const.} - (R^2 - x^2)^{1/2} \approx \text{const.} + x^2/2R$ is the cylinder surface height.

The constant u_0 in (10) can be implicitly calculated with the load balance equation

$$\int_{-\infty}^{\infty} dx' \, p(x') = f_\mathrm{N}, \tag{11}$$

where $f_\mathrm{N} = F_\mathrm{N}/L_\mathrm{y}$ is the cylinder load per unit length. Equations (10) and (11) together with the relation between the interfacial separation and the nominal pressure given by the Persson's contact mechanics theory [29] have to be solved to determine the unknown variables $p(x)$, $u(x)$ and u_0. Here, we use such small surface roughness that it has a negligible influence on the rolling friction result, which is therefore essentially exact.

3 Rolling Friction: Analytical model

If a solid is exposed to a perpendicular surface stress or pressure $p(\mathbf{x},t) = p(\mathbf{x} - \mathbf{v}t)$, a tangential (friction) force will act on the solid given by[25]

$$F_\mathrm{f} = \frac{2(2\pi)^2}{v} \int d^2q \, \frac{\omega}{q} \mathrm{Im} \frac{1}{E_\mathrm{eff}(\omega)} |p(\mathbf{q})|^2, \tag{12}$$

where $\omega = \mathbf{q} \cdot \mathbf{v}$ and $E_\mathrm{eff} = E/(1-\nu^2)$. In principle, ν depends on frequency but the factor $1/(1-\nu^2)$ varies from $4/3 \approx 1.33$ for $\nu = 0.5$ (rubbery region) to ≈ 1.19 for $\nu = 0.4$ (glassy region), and we can neglect the weak dependence on frequency. Within the assumptions given above, Eq. (12) is exact. Note that even if we use $p(\mathbf{q})$ calculated to zero order in $\tan\delta$, the friction force (12) will be correct to linear order in $\tan\delta$. We also note that the present approach is very general and flexible. For example, instead of a semi-infinite solid, the theory is easily generalized to layered materials, e.g., a thin viscoelastic film on a hard flat substrate.

Consider a hard cylinder (radius R and length $L_y \gg R$) rolling on a viscoelastic solid. The same result is obtained during sliding if one assume lubricated contact and if one can neglect the viscous energy dissipation in the lubrication film. When determining the friction force to linear order in $\tan\delta$, we can neglect dissipation in the calculation of the contact pressure $p(x)$, which is therefore described by the Hertz solution. Thus, if we introduce a coordinate system with the y axis parallel to the cylinder axis and with the origin of the x axis in the middle of the contact area (of width $2a$), then the contact stress for $-a < x < a$:

$$p(x) = \frac{2f_N}{\pi a}\left[1 - \left(\frac{x}{a}\right)^2\right]^{1/2}, \tag{13}$$

where $f_N = F_N/L_y$ the load per unit length of the cylinder. The half-width of the contact area in the Hertz contact theory is

$$a = \left(\frac{4f_N R}{\pi E_{\text{eff}}}\right)^{1/2}, \tag{14}$$

where we take E_{eff} to be $|E_{\text{eff}}(\omega)|$ with $\omega = \mathbf{q}\cdot\mathbf{v}$. Substituting the Fourier transform of (13) in (12) and dividing by F_N gives the friction coefficient [25]:

$$\mu_R = \frac{8f_N}{\pi}\int_0^\infty dq_x\ \mathrm{Im}\frac{1}{E_{\text{eff}}(q_x v)}\frac{1}{(aq_x)^2}J_1^2(q_x a), \tag{15}$$

where $J_1(x)$ is the Bessel function of the first kind.

At this point, we empathize that (12) is basically exact, and if one could calculate the contact pressure $p(x)$ [or rather the Fourier transform $p(q_x)$] exactly, then (12) should give the exact result, e.g., the result of Hunter for the cylinder case when assuming the simple viscoelastic modulus consisting of a single term Prony series. Note that the contact pressure will not be symmetric around the midpoint when the dissipation in the rubber is included in the analysis. Still, to linear order in $\tan\delta$, one can neglect this effect [since (12) is explicitly already linear in $\tan\delta$], and the analysis below and in Ref. [25] shows that this is a remarkable accurate approximation, which is an interesting result in its own right, and makes it possible to apply the theory to a wide set of problems.

4 Numerical Results

Here, we compare the results of the numerical procedure developed in Sect. 2 with the predictions of the rolling friction model [25] presented in Sect. 3. Due to the extremely reduced computational requirements of the rolling friction model presented in Sect. 3, with respect to any classical numerical formulation of the viscoelastic contact problem[1], it is of particular interest to quantify the accuracy of the approach presented in Sect. 3 in the case of real rubber rheologies. Indeed, while in the case of (unrealistic) simple rheologies, i.e., characterized by a single relaxation time, the theory is very accurate (see Refs. [25, 26]), there is no proof in the literature of its accuracy for a rheology described by several relaxation times.

We have measured the viscoelastic modulus of an unfilled and filled (with carbon black) nitrile rubber. In Fig. 2, we show for both materials the real and imaginary part of the complex function $1/E(\omega)$ as measured (dots) and

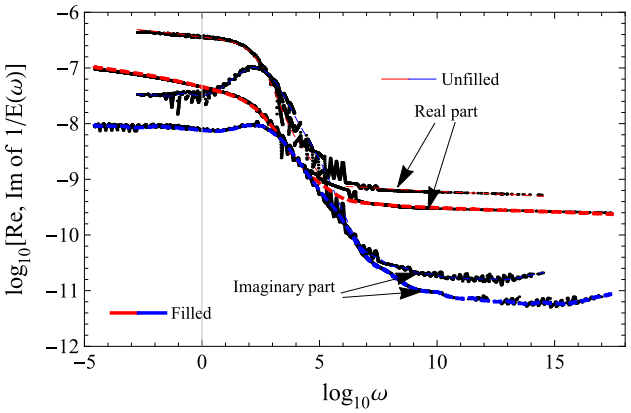

Fig. 2 Real and imaginary part of the complex function $1/E(\omega)$ as measured (*dots*) and fitted by Prony series (*dashed blue and red curves*). For filled (*thick line*) and unfilled rubber. In $\log_{10} - \log_{10}$, with $1/E(\omega)$ in Pa^{-1} and ω in s^{-1}. For the reference temperature, T = 20 °C (Color figure online)

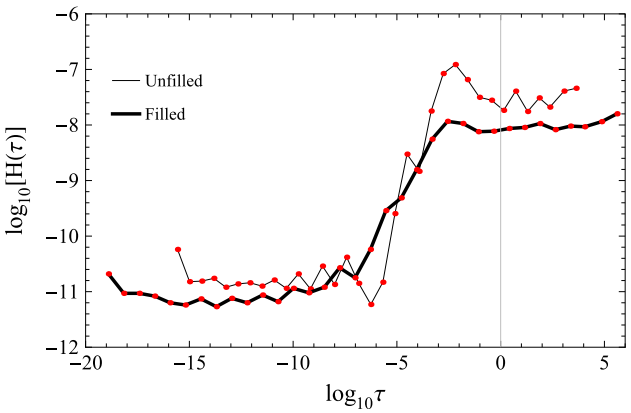

Fig. 3 Spectral density $H(\tau)$ as a function of the relaxation time τ on a $\log_{10} - \log_{10}$ scale. For both filled and unfilled rubber, $H(\tau)$ is Pa^{-1} with τ in s. For the reference temperature, T = 20 °C

[1] It can be easily shown that the discrete formulation of the viscoelastic line contact kernel presents an analytical formulation as it occurs for the elastic case. This largely simplifies the viscoelastic integration.

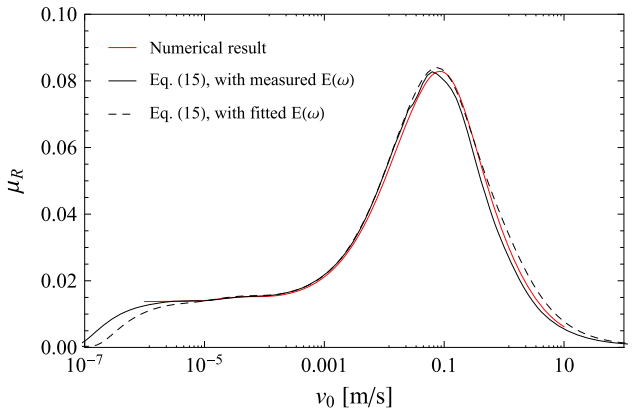

Fig. 4 Rolling friction as a function of the rolling velocity for an unfilled rubber compound, similar to the one described in Fig. 2. For T = 20 °C, $R = 1$ mm and $f_N = 117$ N/m

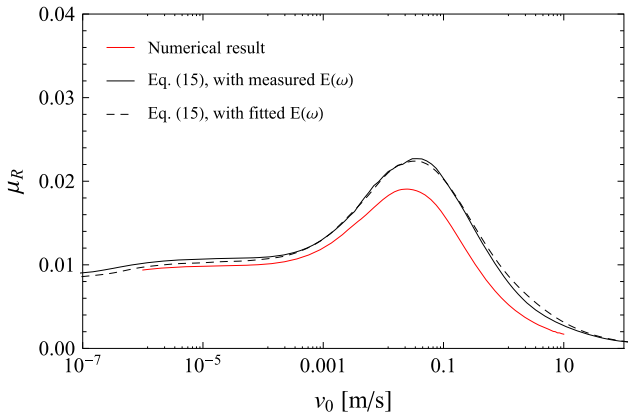

Fig. 5 Rolling friction as a function of the rolling velocity for an filled rubber compound, similar to the one described in Fig. 2. For T = 20 °C, $R = 1$ mm and $f_N = 117$ N/m

fitted by Prony series (dashed blue and red curves) obtained by approximation (6) with:

$$\frac{1}{E(\omega)} \approx \frac{1}{E(\infty)} + \sum_{n=1}^{N} \frac{H(\tau_n)}{1 - i\omega\tau_n},$$

where N is the number of relaxation times. In Fig. 3, we show the spectral density $H(\tau)$ for both the filled and unfilled rubber. Note that the distribution of relaxation times is very wide and cannot be characterized by a simple single relaxation time as often assumed.

In Figs. 4 and 5, we report, respectively, the rolling friction as a function of the sliding velocity for the unfilled and filled rubber compound. In particular, the red curves are calculated from the numerical theory developed in Sect. 2, whereas the black solid and dashed curves represent, respectively, the rolling friction as calculated from the analytical theory (Sect. 3) with the measured complex elastic modulus $E(\omega)$ data and from $E(\omega)$ as calculated from the Prony series fitting of the $1/E(\omega)$ measurements. The latter set of data is also used in the numerical exact theory (red curve).

For the unfilled rubber compound, there is a remarkable agreement between the analytical theory of Sect. 3 and the numerical theory of Sect. 2. For the filled rubber, the match is less accurate, and we suspect that the fitting algorithm has been not perfectly successful to accurately determine the rubber relaxed elastic modulus, which is used in our model in the filled case. Due to the sensibility to such a parameter, this could generate a deviation from the results calculated with the Persson's approach [25]. Indeed, it is well know that rubber with filler particles (e.g., carbon black or silica particles) exhibits a strongly nonlinear viscoelastic response, undergoing strain softening already at a strain of order ~ 1 %. A causal linear response function can be written as a Prony series, but this is not the case when the response is nonlinear (see e.g., [30]). Hence, the analytical model, which makes use of the measured frequency space characterization of the rubber, is expected to provide an accurate rolling friction prediction, almost independently the filling state of the rubber. Differently, we suspect that the accuracy of the numerical model, as well as of all existing models based on the space of time formulation of viscoelasticity, can suffer to some extent of the nonlinearity of the rubber rheology when using Prony series fitting.

For the unfilled sample, in Fig. 6 we show the contact pressure field for some representative values of sliding velocity. The different stages of viscoelastic response are highlighted. The strong asymmetry of the contact pressure fields with respect to the Hertzian shape, prevailing in the rubber transition regime, may suggest a certain restriction of accuracy of Eq. (15) in predicting rolling friction. It would be therefore very interesting to compare $|p(q)|^2 = |f_N J_1(qa)/(\pi qa)|^2$ with respect to the numerically exact results. In particular, in Fig. 7, we show the square of the Fourier transform of the contact pressure (unfilled sample) for representative values of sliding velocities belonging to the rubber transition regime, and corresponding to the pressure curves shown in Fig. 6. Note that all $|p(q)|^2$ curves converge to the same value for $q \approx 0$, as expected since $p(q = 0) = f_N/(2\pi)$. Most interestingly, despite the strong asymmetrical shape of the pressure curves in the transition regime (Fig. 6), in the Fourier space, the inaccuracy resulting from such asymmetry is notably reduced, as expected by previous arguments.

Note that the rolling friction exhibits a very strong temperature dependence (not shown), given by the WLF shift factor a_T: reducing the temperature by 10 °C typically

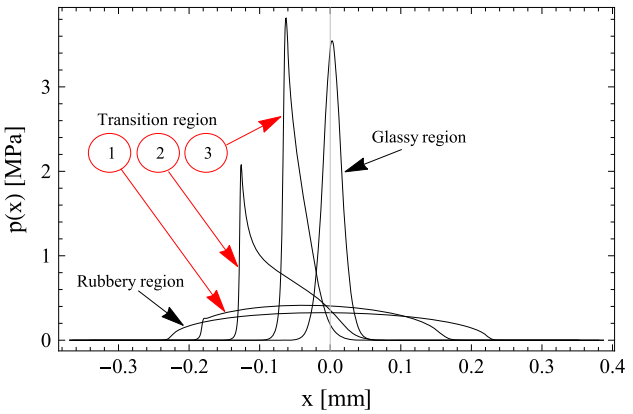

Fig. 6 Contact pressure field for (*1*) $v_0 = 3.0\ mm/s$, (*2*) $v_0 = 77\ mm/s$, (*3*) $v_0 = 0.39\ m/s$. For the unfilled rubber, and for the same parameters of Fig. 4

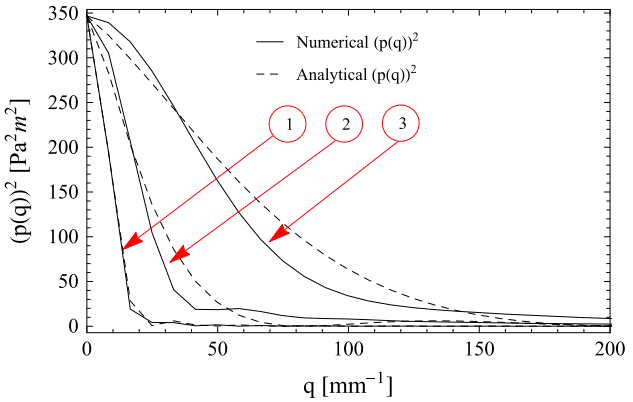

Fig. 7 Square of the Fourier transform of the contact pressure for the unfilled sample. For representative values of sliding velocities belonging to the rubber transition regime and corresponding to the pressure curves shown in Fig. 6

results in a shift of the rolling friction curve toward lower velocities by approximately one decade. At low frequencies (or low rolling velocities), the unfilled rubber is elastically much softer than the filled rubber. Thus, the half-width a_0 of the static Hertz contact region at low rolling velocities is much larger for the unfilled rubber than for the filled rubber. At high rolling velocities, these values becomes much smaller owing to the stiffening of the effective elastic modulus at high frequencies.

5 Summary and Conclusion

We have compared the prediction of an exact numerical study for the rolling friction of a hard cylinder on a smooth flat surface of a viscoelastic solid, with the prediction of an analytical theory. The analytical theory is a very general and flexible approach to calculate the rolling resistance of hard objects on viscoelastic solids. We have shown that to a very good approximation the theory can be applied to *real* rubber materials with *real* complex viscoelastic modulus $E(\omega)$. The theory can be applied to both spheres and cylinders rolling on semi-infinite viscoelastic solids, or on a thin viscoelastic film adsorbed on a rigid flat substrate, or even more complex situations for which the $M_{zz}(\mathbf{q}, \omega)$ -function can be calculated. For a cylinder rolling on a viscoelastic solid characterized by a single relaxation time τ, Hunter has obtained an exact solution for the rolling resistance, and for this limiting case, it was shown already in Ref. [25] that the analytical theory gives almost the same as the result as obtained in the exact treatment. Inversely, the theory can also be adopted to test the accuracy of the fitting process used to determine, from the measured complex elastic modulus, the terms describing the Prony series (e.g., the relaxed elastic modulus), as usually required by the viscoelastic calculations made in the space of lengths.

Acknowledgments We thank K.W. Stöckelhuber and G. Heinrich (Leibniz-Institut für Polymerforschung, Dresden) for supplying the nitrile rubber and B. Lorenz (FZJ) for measuring the viscoelastic modulus. MS acknowledges FZJ for the support and the kind hospitality received during his visit to the PGI-1, where this work has been performed. MS also acknowledges COST Action TD0906 for grants STSM-TD0906-020613-031727 and STSM-TD0906-230413-030252.

References

1. Persson, B.: Sliding Friction: Physical Principles and Applications, 2nd edn. Springer, Heidelberg (2000)
2. Grosch, K.: The relation between the friction and visco-elastic properties of rubber. Proc. R. Soc. Lond. A Mat. **274**, 21–39 (1963)
3. Persson, B.: Theory of rubber friction and contact mechanics. J. Chem. Phys. **22**, 325107 (2010)
4. Persson, B.: Rubber friction: role of the flash temperature. J. Phys.: Condens. Matter **18**, 7789–7823 (2006)
5. Persson, B., Albohr, O., Tartaglino, U., Volokitin, A., Tosatti, E.: On the nature of surface roughness with application to contact mechanics, sealing, rubber friction and adhesion. J. Phys.: Condens. Matter **17**, R1–R62 (2005)
6. Heinrich, G., Klüppel, M., Vilgis, T.: Evaluation of self-affine surfaces and their implication for frictional dynamics as illustrated with a Rouse material. Comput Theory Polym S **10**, 53–61 (2000)
7. Heinrich, G., Klüppel, M.: Rubber friction, tread deformation and tire traction. Wear **265**, 1052–1060 (2008)
8. Persson, B., Volokitin, A.: Rubber friction on smooth surfaces. Eur. Phys. J. E **21**, 69–80 (2006)
9. Carbone, G., Lorenz, B., Persson, B., Wohlers, A.: Contact mechanics and rubber friction for randomly rough surfaces with anisotropic statistical properties. Eur. Phys. J. E **29**, 275–284 (2009)
10. Persson, B.: On the theory of rubber friction. Surf. Sci. **401**, 445–454 (1998)

11. Le Gal, A., Yang, X., Klüppel, M.: Evaluation of sliding friction and contact mechanics of elastomers based on dynamic-mechanical analysis. J. Chem. Phys. **123**, 014704 (2005)
12. Persson, B.: Theory of powdery rubber wear. J. Phys.: Condens. Matter **21**, 485001 (2009)
13. Mofidi, M., Prakash, B., Persson, B., Albohr, O.: Rubber friction on (apparently) smooth lubricated surfaces. J. Phys. Condens. Mat. **20**, 085223 (2008)
14. Persson, B., Albohr, O., Creton, C., Peveri, V.: Contact area between a viscoelastic solid and a hard, randomly rough, substrate. J. Chem. Phys. **120**, 8779–8793 (2004)
15. Greenwood, J., Johnson, K., Choi, S.-H., Chaudhury, M.: Investigation of adhesion hysteresis between rubber and glass using a pendulum. J. Phys. D: Appl. Phys. **42**, 035301 (2009)
16. She, H., Malotky, D., Chaudhury, M.: Estimation of Adhesion Hysteresis at Polymer/Oxide Interfaces Using Rolling Contact Mechanics. Langmuir **14**, 3090–3100 (1998)
17. Greenwood, J., Tabor, D.: The friction of hard sliders on lubricated rubber: the importance of deformation losses. J. Phys. Soc. **71**, 989 (1958)
18. Greenwood, J.A., Minshall, H., Tabor, D.: Hysteresis losses in rolling and sliding friction. Proc R. Soc. Lond. A Mat. **259**, 480–507 (1961)
19. Tabor, D.: The rolling and skidding of automobile tyres. Phys. Rev. Spec. Top-Ph **29**, 301 (1994)
20. Felhos, D., Xu, D., Schlarb, A., Vradi, K., Goda, T.: Viscoelastic characterization of an EPDM rubber and finite element simulation of its dry rolling friction. Express Polym. Lett. **2**, 157–164 (2008)
21. Hunter, S.: The rolling contact of a rigid cylinder With a viscoelastic half space. J. Appl. Mech. **28**, 611–617 (1961)
22. Goryacheva, I.G.: Contact problem of rolling of a viscoelastic cylinder on a base of the same material. J. Appl. Math. Mech. **37** 877–885 (1973)
23. Panek, C., Kalker, J.: Three-dimensional contact of a rigid roller traversing a viscoelastic half space. IMA. J. Appl. Math. **26**, 299–313 (1980)
24. Vollebregt, E.: User guide for CONTACT, Vollebregt and Kalker's rolling and sliding contact model. Techical report TR09-03, version 13.1 (2013)
25. Persson, B.: Rolling friction for hard cylinder and sphere on viscoelastic solid. Eur. Phys. J. E **33**, 327–333 (2010)
26. Carbone, G., Putignano, C.: A novel methodology to predict sliding and rolling friction of viscoelastic materials: theory and experiments. J. Mech. Phys. Solids **61**, 1822–1834 (2013)
27. Persson, B.: Contact mechanics for layered materials with randomly rough surfaces. J. Phys. Condens. Mat. **24**, 095008 (2012)
28. Scaraggi, M., Persson, B.: Theory of viscoelastic lubrication. Tribol Int **72**, 118–130 (2014)
29. Yang, C. Persson, B.: Contact mechanics: contact area and interfacial separation from small contact to full contact. J. Phys. Condens. Mat. **20**, 215214 (2008)
30. Lorenz, B., Pyckhout-Hintzen, W., Persson, B.: Master curve of viscoelastic solid: using causality to determine the optimal shifting procedure, and to test the accuracy of measured data. Polymer **55**, 565–571 (2014)